Thermal limit to the intrinsic emittance from metal photocathodes

Jun Feng, J. Nasiatka, Weishi Wan, Siddharth Karkare, John Smedley, and Howard A. Padmore

Citation: Applied Physics Letters **107**, 134101 (2015); doi: 10.1063/1.4931976
View online: http://dx.doi.org/10.1063/1.4931976
View Table of Contents: http://scitation.aip.org/content/aip/journal/apl/107/13?ver=pdfcov
Published by the AIP Publishing

Thermal limit to the intrinsic emittance from metal photocathodes

Jun Feng,[1,a)] J. Nasiatka,[1] Weishi Wan,[1] Siddharth Karkare,[1] John Smedley,[2] and Howard A. Padmore[1]
[1]*Lawrence Berkeley National Laboratory, Berkeley, California 94720, USA*
[2]*Brookhaven National Laboratory, Upton, New York 11973, USA*

(Received 29 July 2015; accepted 17 September 2015; published online 28 September 2015)

Measurements of the intrinsic emittance and transverse momentum distributions obtained from a metal (antimony thin film) photocathode near and below the photoemission threshold are presented. Measurements show that the intrinsic emittance is limited by the lattice temperature of the cathode as the incident photon energy approaches the photoemission threshold. A theoretical model to calculate the transverse momentum distributions near this photoemission threshold is presented. An excellent match between the experimental measurements and the theoretical calculations is demonstrated. These measurements are relevant to low emittance electron sources for Free Electron Lasers and Ultrafast Electron Diffraction experiments. © *2015 AIP Publishing LLC*.
[http://dx.doi.org/10.1063/1.4931976]

Photoinjectors are the preferred sources of electrons for most 4th generation light sources such as energy recovery lincas and free electron lasers, and for ultra-fast electron diffraction (UED) setups.[1–4] The performance of these applications depends on the emittance of the electron beam delivered by the photoinjector. Smaller emittance results in brighter electron beams for light sources[1,2] and longer transverse coherence lengths for UED applications.[3,4] The emittance obtained from photoinjectors is limited by the intrinsic emittance of the electron beam emitted from the photocathode.[5,6] Assuming no correlation between the transverse position and the transverse momentum of the electrons at the cathode surface, the intrinsic emittance is given by[7]

$$\epsilon_x = \frac{\sigma_x}{m_e c}\sqrt{\langle p_x^2\rangle}, \tag{1}$$

where m_e is the mass of a free electron, c is the speed of light, (σ_x) is the rms laser spot size on the cathode and p_x is the momentum of the emitted electrons in the transverse (x) direction. For a given electric field at the cathode, the minimum value of the laser spot size is determined by the electron bunch charge required for the application leaving reduction in the transverse momentum of the emitted electrons as the only route to lower intrinsic emittance.[5]

The mean squared transverse momentum ($\langle p_x^2\rangle$) depends on the photocathode material and the photon energy of the incident light.[8] Following the three step model of photoemission, Dowell and Schmerge[9] obtained the mean squared transverse momentum in terms of the photocathode work function and the incident photon energy as

$$\frac{\langle p_x^2\rangle}{m_e} = \frac{\hbar\omega - \phi}{3}, \tag{2}$$

where $\hbar\omega$ is the incident photon energy, and ϕ is the work function of the photocathode and their difference $(\hbar\omega - \phi)$ is called the excess energy. The derivation of Equation (2) assumes a Heaviside step function as the electron state occupation function and a constant density of states. Despite these assumptions, Equation (2) explains experimental data obtained from metallic[10] and alkali-antimonide cathodes[11–13] when the excess energy is much larger than the thermal energy, k_BT (where k_B is the Boltzmann constant and T is the cathode temperature). This theory predicts that $\langle p_x^2\rangle$ should become arbitrarily small as the excess energy goes to zero. However, this theory fails when the excess energy becomes comparable to or lower than the thermal energy, i.e., when the photon energy is very close to the photoemission threshold. Furthermore, there is no experimental data available for the transverse momentum distribution near the photoemission threshold of metals.

In this paper, we present measurements of transverse momentum distributions obtained from a metal (thin Sb film) as a function of the photon energy near and below the photoemission threshold. Further, we extend Dowell and Schmerge's theory to include the effects of a realistic electron occupation function (Fermi function) and a realistic density of states. We show that $\langle p_x^2\rangle$ approaches k_BTm_e as the photon energy approaches k_BT, thus limiting the smallest achievable intrinsic emittance. We find that the transverse momentum distributions predicted by this modified Dowell's theory agree perfectly with the measured distributions.

The Sb film was deposited on a Mo plug at room temperature by thermal evaporation of Sb beads. The thickness of the film was estimated to be 30 nm using a quartz microbalance. The work function of the deposited Sb film was found to be 4.5 eV by measuring the photoelectron yield as a function of photon energy.[14] The base pressure in the deposition chamber was less than 10^{-9} Torr. The sample was then transferred into the transverse momentum distribution measurement system in vacuum.

In the transverse momentum distribution measurement system, the light from a high brightness laser driven UV-visible light source[15] is focused to a 150 μm FWHM spot on the sample (the cathode). The electrons emitted from this spot are accelerated towards a flat parallel grid (the anode)

a)Electronic mail: fjun@lbl.gov

located at a distance of 3 mm from the sample. A grid of 25 μm spacing is used. The beam of light is incident on the sample after passing through the grid. The diffraction pattern formed on the sample due to the grid is smaller than the spot size and can be ignored. An acceleration voltage of 3–6 kV is applied to the cathode and the grid is grounded. The electrons passing through the grid have a high kinetic energy (3–6 kV) and form a beam which is allowed to drift in a field free region while expanding in the transverse direction due to the transverse momenta of the emitted electrons. The cross section of the beam is then imaged using an MCP (Micro Channel Plate)-phosphor screen assembly located at a distance of 269 mm from the grid. The transverse momentum of the electron at a displacement L (in the x direction) from the center of the spot measured on the phosphor screen is given by

$$p_x = \frac{L}{2g+d}\sqrt{2m_e eV}, \tag{3}$$

where g is the gap between the cathode and the grid, d is the drift length between the grid and the MCP-phosphor screen assembly, e is the electron charge, and V is the accelerating voltage. Thus, the transverse momentum distribution can be obtained from the image of the electron beam on the phosphor screen. In Equation (3), it appears that the transverse momentum has a square root dependence on the voltage V. However, the beam size L has an inverse square root dependence on the voltage and they cancel out to make the transverse momentum independent of the accelerating voltage. The electron beam currents used are small enough for the space charge to be negligible. The details of this setup and the measurement technique can be found elsewhere.[16]

Figure 1 shows the electron beam cross section imaged on the phosphor screen for incident photon energies of 4.77 eV and 4.43 eV at accelerating voltages of 3 kV and 6 kV. Figure 2 shows the momentum distributions obtained from the images shown in Figure 1 using Equation (3). The momentum distributions obtained at 3 kV and 6 kV are identical, re-enforcing the validity of the measurement technique. Figure 3 shows the variation of the intrinsic emittance (or equivalently $\langle p_x^2 \rangle$) with the excess energy ($\hbar\omega - \phi$), assuming a rms laser spot size (σ_x) of 1 mm. We can see that the emittance reduces with excess energy at higher values of excess energy but flattens out to a value of 0.23 μm as the excess energy approaches zero. This corresponds to $\frac{\langle p_x^2 \rangle}{m_e} = 25.9$ meV, which is same as the thermal energy at room temperature.

In order to explain these results, we extended Dowell and Schmerge's theory to include the effects of the non-zero width of the Fermi distribution and a realistic density of states. As shown by Dowell,[9] the number of electrons emitted is proportional to

$$N_e = \int_{\epsilon}^{\infty} dE f(E) N(E) \int_{\cos\theta_m}^{1} d(\cos\theta) \int_{0}^{2\pi} d\Phi, \tag{4}$$

where $\epsilon = E_f + \phi - \hbar\omega$, E_f is the Fermi energy, θ is the angle made by the incoming electron with the surface normal (polar angle), θ_m is the maximum polar angle at which the electrons can still be emitted, Φ is the azimuthal angle, $f(E)$ is the electron occupation function, and $N(E)$ is the density of states. In this work, we use the Fermi function as the electron occupation function to accurately model the photoemission near threshold. Hence, $f(E) = 1/\left(1 + e^{\frac{E-E_f}{k_B T}}\right)$. By transforming the coordinates in Equation (4), N_e can be written in terms of the energy E and the two transverse momenta p_x and p_y as

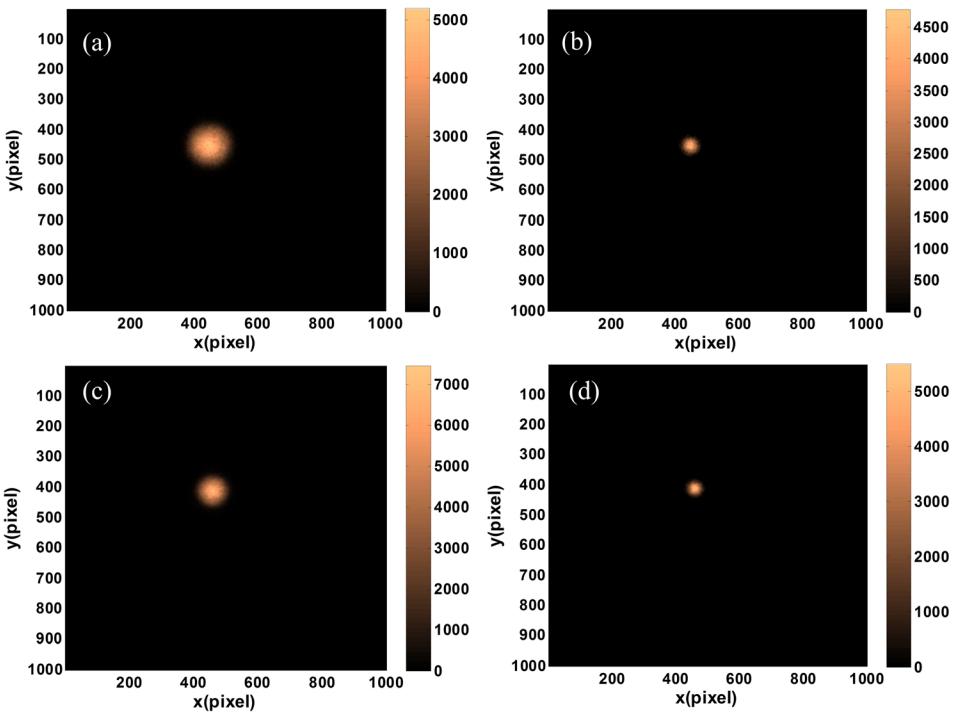

FIG. 1. Measured electron beam image from a Sb film deposited on a Mo plug on the phosphor screen by CCD camera. (a) 3 kV accelerating voltage and 260 nm incident light. (b) 3 kV accelerating voltage and 280 nm incident light. (c) 6 kV accelerating voltage and 260 nm incident light. (d) 6 kV accelerating voltage and 280 nm incident light. The scale on the color bars is in arbitrary units. One pixel corresponds to 0.035 mm.

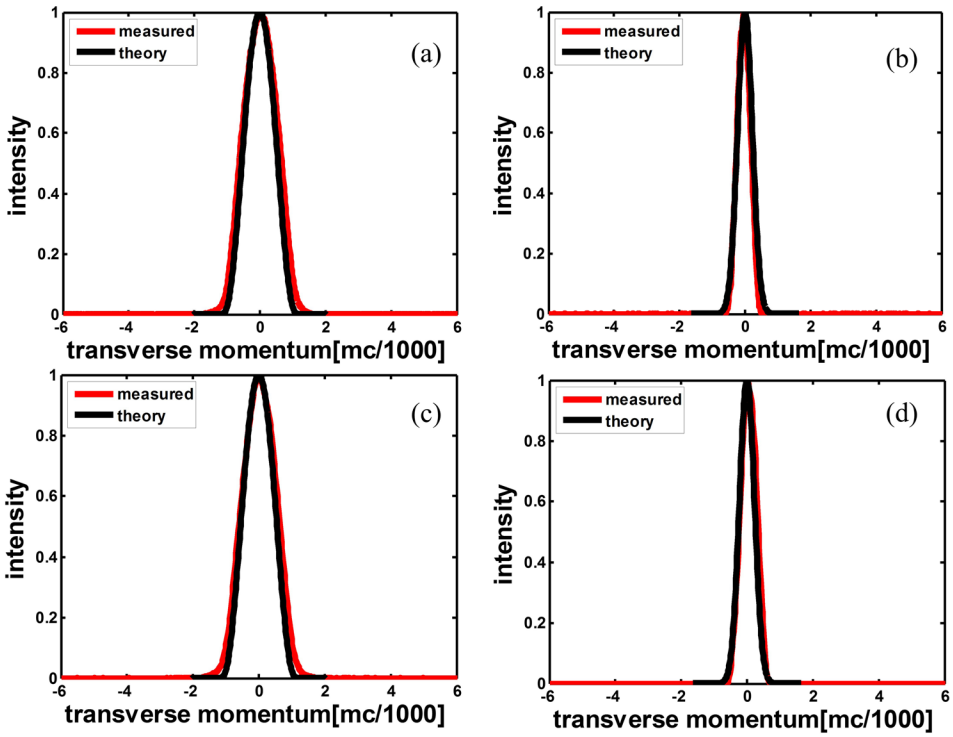

FIG. 2. Transverse momentum distributions from a Sb film deposited on a Mo plug. The momentum distributions are obtained using Equation (3) and the electron beam images shown in Figure 1 (a) 3 kV accelerating voltage and 260 nm incident light. (b) 3 kV accelerating voltage and 280 nm incident light. (c) 6 kV accelerating voltage and 260 nm incident light. (d) 6 kV accelerating voltage and 280 nm incident light.

$$N_e = \int_{-\infty}^{\infty} dp_x \int_{E_{min}}^{\infty} dE \frac{f(E)N(E)}{\sqrt{2m_eE}} \times \int_{-\sqrt{p_{\|M}^2 - p_x^2}}^{\sqrt{p_{\|M}^2 - p_x^2}} dp_y \frac{1}{\sqrt{2m_eE - p_x^2 - p_y^2}}, \quad (5)$$

where $E_{min} = \frac{p_x^2}{2m_e} + \epsilon$ and $p_{\|M} = \sqrt{2m_e(E-\epsilon)}$. Integrating over p_y in Equation (5) and differentiating w.r.t p_x, we obtain the expression for the transverse momentum distribution in the x direction as

$$\frac{dN_e}{dp_x} = C \int_{E_{min}}^{\infty} dE \frac{f(E)N(E)}{\sqrt{2m_e(E+\hbar\omega)}} \times \arcsin\left(\sqrt{\frac{2m_e(E-\epsilon) - p_x^2}{2m_e(E+\hbar\omega) - p_x^2}}\right), \quad (6)$$

where C is a constant of proportionality.

The transverse momentum distributions for two photon energies $\hbar\omega = 4.77$ eV and 4.43 eV were calculated by numerically integrating the expression in Equation (6). Work function ϕ was assumed to be 4.5 eV and the density of states $N(E)$ was assumed to be constant. The calculated transverse momentum distributions are shown in Figure 2. An exact match with the experimental distributions was obtained.

The mean squared transverse momentum can be calculated as

$$\langle p_x^2 \rangle = m_e \frac{\int_{\epsilon}^{\infty} dE f(E)N(E) \int_{\cos\theta_m}^{1} d(\cos\theta) \int_0^{2\pi} d\Phi p_x^2}{\int_{\epsilon}^{\infty} dE f(E)N(E) \int_{\cos\theta_m}^{1} d(\cos\theta) \int_0^{2\pi} d\Phi}. \quad (7)$$

Integrating over the polar and azimuthal angles as done by Dowell and Schmerege,[9] we obtain

$$\langle p_x^2 \rangle = \frac{m_e \int_{\epsilon}^{\infty} dE \frac{N(E)(E+\hbar\omega)}{1+e^{(E-E_f)/k_BT}} \left[\frac{2}{3} - \sqrt{\frac{E_f+\phi}{E+\hbar\omega}} + \frac{1}{3}\left(\frac{E_f+\phi}{E+\hbar\omega}\right)^{\frac{3}{2}}\right]}{\int_{\epsilon}^{\infty} dE \frac{N(E)}{1+e^{(E-E_f)/k_BT}} \left(1 - \sqrt{\frac{E_f+\phi}{E+\hbar\omega}}\right)}. \quad (8)$$

It is not possible to calculate the integrals in Equation (8) analytically; however, in the limiting case of $\phi > \phi - \hbar\omega \gg k_BT$, i.e., when the photon energy is well below the photoemission threshold and photoemission occurs only from the Fermi tail, one can show $\langle p_x^2 \rangle \to m_e k_B T$, assuming the density of states $N(E)$ is constant. This limit corresponds to an

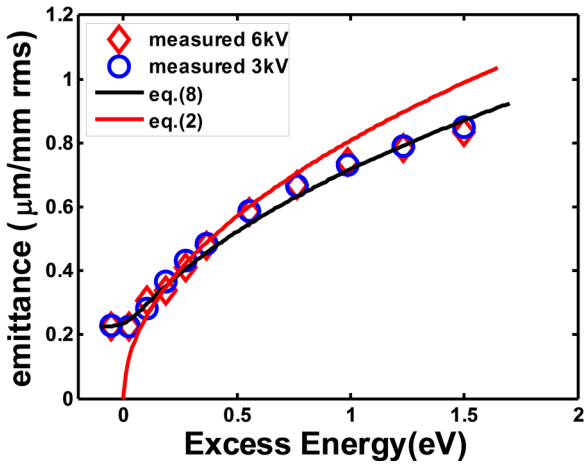

FIG. 3. Transverse emittance as a function of excess energy for a Sb film measured at 3 kV and 6 kV accelerating voltages with a comparison with theory (Equation (8)). The results obtained from Dowell's theory (Equation (2)) are also shown for comparison. The excess energy is varied by changing the photon energy.

emittance of 0.23 μm for a rms laser spot size of 1 mm. The experimental data presented in Figure 3 indeed shows that this limit has been reached.

$\langle p_x^2 \rangle$ was calculated for various photon energies by numerically evaluating the integrals in Equation (8). The density of states obtained experimentally using XPS[17] was used. The results of the calculation as a function of the excess energy are presented in Figure 3. It is important to note that the calculation presented here does not involve any *ad hoc* parameters. The perfect match obtained between the experiment and this modified Dowell's theory is noteworthy. It is important to include the variation in the density of states in order to obtain this excellent fit, especially at excess energies greater than 0.5 eV. The density of states is the only material dependent parameter used in the theory. Since the variation in the density of states is very small near the threshold, the limit of $m_e k_B T$ for the mean squared transverse momentum should be applicable for all metals.

This theory and measurements suggest that reducing the lattice temperature of the cathode is a possible route to reducing the intrinsic emittance of metal cathodes near threshold. Such a reduction has been experimentally demonstrated for near threshold photoemission in alkali-antimonide semiconductor cathodes, however the thermal limit was not observed because of other factors like surface non-uniformities and non-uniform density of states near the threshold.[18,19]

In conclusion, we have made measurements of the transverse momentum distributions obtained from a metal (Sb thin film) near the photoemission threshold. The measurements show that the minimum intrinsic emittance attainable from metal photocathodes is limited by the lattice temperature of the cathode. Finally, we develop a theory to calculate the transverse momentum distributions and the intrinsic emittance of metal photocathodes near the photoemission threshold and show that the calculations perfectly match the measured values. Up to this point most simulations of beam dynamics in photoinjectors have assumed a Maxwellian transverse velocity distribution of the photoelectrons leaving the photocathode.[5] We have derived an exact shape for the distribution which will be helpful in accurate simulations of photoinjectors and other applications.

The authors would like to thank Jared Wong, Susanne Schubert, and Xumin Chen for rewarding discussion. This work was performed at LBNL under the auspices of the Office of Science, Office of Basic Energy Sciences, of the U.S. Department of Energy under Contract Nos. DE-AC02-05CH11231, KC0407-ALSJNT-I0013, and DE-SC0005713.

[1]S. M. Gruner, D. Bilderback, I. Bazarov, K. Finkelstein, G. Krafft, L. Merminga, H. Padamsee, Q. Shen, C. Sinclair, and M. Tigner, Rev. Sci. Instrum. **73**, 1402 (2002).
[2]W. Ackermann, G. Asova, V. Ayvazyan, A. Azima, N. Baboi, J. Bahr, V. Balandin, B. Beutner, A. Brandt, A. Bolzmann *et al.*, Nat. Photonics **1**, 336 (2007).
[3]P. Musumeci, J. T. Moody, C. M. Scoby, M. S. Gutierrez, H. A. Bender, and N. S. Wilcox, Rev. Sci. Instrum. **81**, 013306 (2010).
[4]T. van Oudheusden, E. F. de Jong, S. B. van der Geer, W. P. E. M. O. Root, O. J. Luiten, and B. J. Siwick, J. Appl. Phys. **102**, 093501 (2007).
[5]I. V. Bazarov, B. M. Dunham, and C. K. Sinclair, Phys. Rev. Lett. **102**, 104801 (2009).
[6]C. Gulliford, A. Bartnik, I. Bazarov, L. Cultrera, J. Dobbins, B. Dunham, F. Gonzalez, S. Karkare, H. Lee, H. Li *et al.*, Phys. Rev. Spec. Top. Accel. Beams. **16**, 073401 (2013).
[7]I. V. Bazarov, B. M. Dunham, Y. Li, X. Liu, D. G. Ouzounov, C. K. Sinclair, F. Hannon, and T. Miyajima, J. Appl. Phys. **103**, 054901 (2008).
[8]D. H. Dowell, I. Bazarov, B. Dunham, K. Harkay, C. Hernandez-Garcia, R. Legg, H. Padmore, T. Rao, J. Smedley, and W. Wan, Nucl. Instrum. Methods Phys. Res., Sect. A **622**, 685 (2010).
[9]D. Dowell and J. Schmerge, Phys. Rev. Spec. Top. Accel. Beams **12**, 074201 (2009).
[10]C. P. Hauri, R. Ganter, F. L. Pimpec, A. Trisorio, C. Ruchert, and H. H. Braun, Phys. Rev. Lett. **104**, 234802 (2010).
[11]L. Cultrera, I. Bazarov, A. Bartnik, B. Dunham, S. Karkare, R. Merluzzi, and M. Nichols, Appl. Phys. Lett. **99**, 152110 (2011).
[12]I. Bazarov, L. Cultrera, A. Bartnik, B. Dunham, S. Karkare, Y. Li, X. Liu, J. Maxson, and W. Roussel, Appl. Phys. Lett. **98**, 224101 (2011).
[13]T. Vecchione, I. Ben-Zvi, D. H. Dowell, J. Feng, T. Rao, J. Smedley, W. Wan, and H. A. Padmore, Appl. Phys. Lett. **99**, 034103 (2011).
[14]R. Fowler, Phys. Rev. **38**, 45 (1931).
[15]J. Feng, J. Nasiatka, J. Wong, X. Chen, S. Hidalgo, T. Vecchione, H. Zhu, F. J. Palomares, and H. A. Padmore, Rev. Sci. Instrum. **84**, 085114 (2013).
[16]J. Feng, J. Nasiatka, W. Wan, T. Vecchione, and H. A. Padmore, Rev. Sci. Instrum. **86**, 015103 (2015).
[17]D. Bullet, Solid State Commun. **17**, 965 (1975).
[18]J. Maxson, L. Cultrera, C. Gulliford, and I. Bazarov, Appl. Phys. Lett. **106**, 234102 (2015).
[19]L. Cultrera, S. Karkare, H. Lee, X. Liu, I. Bazarov, and B. Dunham, e-print arXiv:1504.05920.